Article

Cell Reports

Sox9 Activation Highlights a Cellular Pathway of Renal Repair in the Acutely Injured Mammalian Kidney

Graphical Abstract

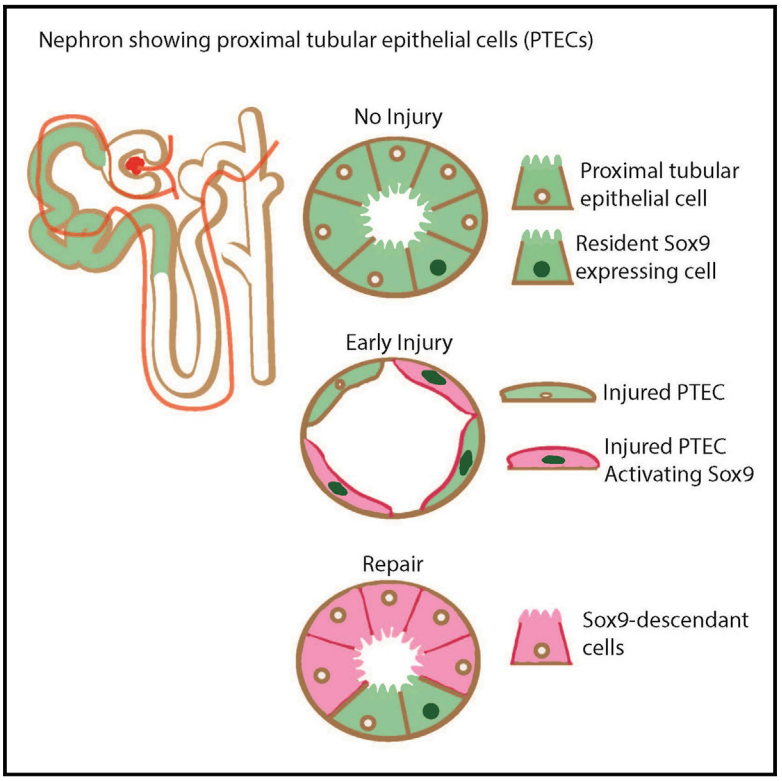

Highlights

- Sox9 activation is an early transcriptional response to acute kidney injury (AKI)
- Sox9-descendant cells regenerate functional proximal tubular epithelium after AKI
- Sox9 is required for a normal epithelial repair process after AKI

Authors

Sanjeev Kumar, Jing Liu, Paul Pang, ..., Andreas Schedl, Benjamin D. Humphreys, Andrew P. McMahon

Correspondence

amcmahon@med.usc.edu

In Brief

Surviving tubular epithelial cells repair the nephron after acute kidney injury (AKI). Kumar et al. identify Sox9 activation as a rapid response to AKI within repairing cells of the damaged proximal tubule segment. Sox9 activation is required for a normal repair process.

Kumar et al., 2015, Cell Reports *12*, 1325–1338
August 25, 2015
http://dx.doi.org/10.1016/j.celrep.2015.07.034

CellPress

Cell Reports
Article

Sox9 Activation Highlights a Cellular Pathway of Renal Repair in the Acutely Injured Mammalian Kidney

Sanjeev Kumar,[1] Jing Liu,[1] Paul Pang,[1] A. Michaela Krautzberger,[1] Antoine Reginensi,[2] Haruhiko Akiyama,[3] Andreas Schedl,[2] Benjamin D. Humphreys,[4] and Andrew P. McMahon[1,*]
[1]Department of Stem Cell Biology and Regenerative Medicine, Eli and Edythe Broad-CIRM Center for Regenerative Medicine and Stem Cell Research, W.M. Keck School of Medicine, University of Southern California, Los Angeles, CA 90089, USA
[2]INSERM U636, Universite de Nice-Sophia Anitpolis, Centre de Biochimie, Parc Valrose, 06108 Nice Cedex 02, France
[3]Department of Orthopedics, Gifu University, Gifu 501-1194, Japan
[4]Renal Division, Brigham and Women's Hospital and Department of Medicine, Harvard Medical School, Boston, MA 02115, USA
*Correspondence: amcmahon@med.usc.edu
http://dx.doi.org/10.1016/j.celrep.2015.07.034

SUMMARY

After acute kidney injury (AKI), surviving cells within the nephron proliferate and repair. We identify Sox9 as an acute epithelial stress response in renal regeneration. Translational profiling after AKI revealed a rapid upregulation of *Sox9* within proximal tubule (PT) cells, the nephron cell type most vulnerable to AKI. Descendants of Sox9$^+$ cells generate the bulk of the nephron during development and regenerate functional PT epithelium after AKI-induced reactivation of Sox9 after renal injury. After restoration of renal function post-AKI, persistent Sox9 expression highlights regions of unresolved damage within injured nephrons. Inactivation of *Sox9* in PT cells pre-injury indicates that *Sox9* is required for the normal course of post-AKI recovery. These findings link *Sox9* to cell intrinsic mechanisms regulating development and repair of the mammalian nephron.

INTRODUCTION

The clinical syndrome of acute kidney injury (AKI) is characterized by an abrupt decline in kidney function, leading to the accumulation of toxic waste products of cellular metabolism and derangement of electrolyte balance. AKI is frequently initiated by ischemia reperfusion injury (IRI), as might occur on organ transplant, and a variety of other insults such as sepsis, nephrotoxic agents, and blockage of urinary flow (Abuelo, 2007). Proximal tubular epithelial cells (PTECs) within the nephron exhibit high metabolic activity and are the most vulnerable cell type to these varied insults in most mammalian species, though distal tubular epithelial cells are also affected in man (Oberbauer et al., 1999; Bonventre and Yang, 2011). Despite advances in medical care, AKI is associated with a significant increase in morbidity and mortality, with in-hospital mortality rates approaching 50%–70% (Chertow et al., 2005). Moreover, survivors of an episode of AKI show an enhanced risk of long-term progression to chronic kidney disease (CKD) and ultimately end-state renal disease (ESRD; Coca et al., 2012).

In AKI, damage-invoking responses trigger necrotic and/or apoptotic cell death depending upon the severity of injury and initiate endogenous tubular repair. This process restores tubular epithelial integrity, proximal tubule activity, and kidney function over several days (Bonventre and Yang, 2011). Genetic fate-mapping studies in the mouse suggest that intrinsic, surviving tubular epithelial cells proliferate and repair damaged nephrons (Humphreys et al., 2008). Whether all surviving epithelial cells have similar replicative/repair capability or a distinct subset of surviving epithelial cells effect repair on injury is not clear (Berger and Moeller, 2014; Kumar et al., 2014; Smeets et al., 2013). While there is good evidence from genetic cell labeling studies of terminally differentiated cell types for the former mechanism (Kusaba et al., 2014), other studies have argued for rare reparative stem/progenitor cell types in the mouse and human kidney (Lazzeri et al., 2007; Lindgren et al., 2011; Rinkevich et al., 2014; Romagnani, 2011). Importantly, the molecular drivers of the intrinsic PTEC proliferative/repair responses post-injury have not been identified. Further, the elevated risk of CKD points to potential limitations in the normal repair processes (Chawla et al., 2014; Kumar et al., 2014). Identifying the kidney's intrinsic mechanisms of repair is critical for developing novel regenerative strategies to treat renal injury.

Recently, our laboratory applied translating ribosome affinity purification (TRAP) methodology within an IRI-induced AKI model to determine the translatome of distinct cell lineages after renal injury in the mouse (Liu et al., 2014)). These studies identified activation of *Sox9,* a member of the Sry-related high-mobility group box of transcription factors (Wright et al., 1993), as an early injury response signature within the nephron population.

Sox9 plays a pivotal role in development of a number of cell types and organ systems; for example, *Sox9* activity is essential for male sex determination and mammalian skeletal development (Wagner et al., 1994). In the kidney, *Sox9* and the closely related family member *Sox8* have redundant activities in the control of branching morphogenesis in the arborizing network of the urinary transport system (Reginensi et al., 2011). *Sox9* is also

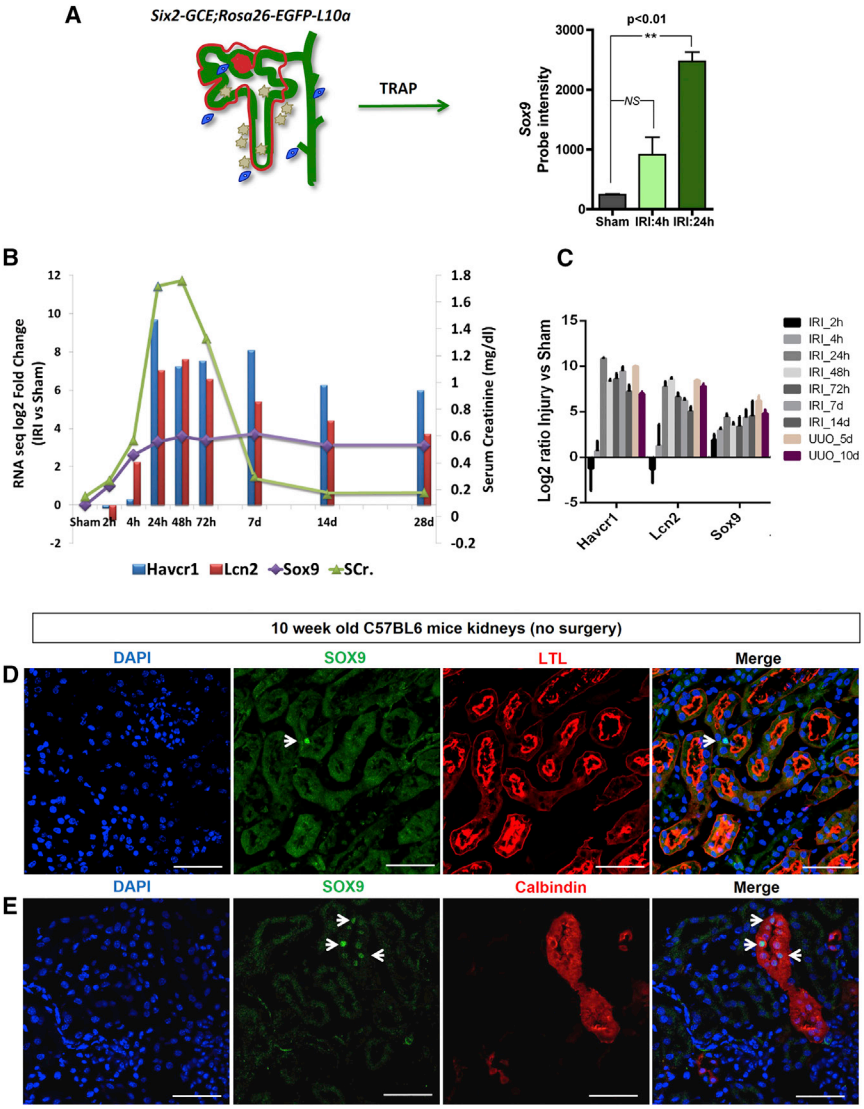

Figure 1. *Sox9* Is Upregulated in the Proximal Tubules Early after Acute Kidney Injury

(A) TRAP microarray analysis of Sox9 levels in *Six2-Tet-GFP-Cre;Rosa26-EGFP-L10a*-labeled nephrons 4 and 24 hr after renal ischemia reperfusion injury (IRI). Mean ± SEM (*NS*, non-significant; $^{**}p < 0.01$, n = 3 mice/group).

(B) RNA sequencing (RNA-seq)-based temporal comparative profile of *Sox9*, *Havcr1*, and *Lcn2* transcript levels at varying times post-IRI (data minimum three mice per group). Serum creatinine levels at corresponding time points are displayed (mean ± SEM; n = 6–8 mice/group).

(C) Fluidigm qPCR temporal analysis of *Sox9*, *Havcr1*, and *Lcn2* levels in response to renal IRI and unilateral ureteral obstruction (UUO).

(D and E) Immunoanalysis for SOX9, LTL (lotus tetragonolobus lectin, proximal tubule) and calbindin (Calbindin-D28K, distal convoluted tubule) in the 10-week adult C57BL6 kidney. DAPI demarcates nuclei. Arrows highlight $SOX9^+$ cells. Data are a minimum of three mice/group. Scale bar, 100 μm. See also Figure S1.

RESULTS

Sox9 Activation on Kidney Injury

To identify cell-type-specific responses after ischemia reperfusion injury (IRI) in an acute kidney injury (AKI) model, we performed translating ribosome affinity purification (TRAP; Liu et al., 2014). Examining the nephron tubular compartment 4 and 24 hr after renal IRI highlighted a marked Sox9 upregulation implicating Sox9-mediated transcriptional regulation in the early response to tubular injury (Figure 1A).

To examine the *Sox9* response in more detail, we compared the *Sox9* expression profile from whole-kidney RNA-sequencing (RNA-seq) of adult male mice subjected to bilateral renal IRI, an AKI model compatible with survival for at least 1 year post-IRI, to kidneys from sham surgery control animals (Figure 1B). In this, model, a rise of serum creatinine levels (peaking 48–72 hr post-IRI) and restoration of basal creatinine levels 14–28 days post-IRI provide an indirect physiological measure of renal injury and repair (Figure 1B). Injury is associated with a dramatic elevation of *Lcn2* (Mishra et al., 2003) and *Havcr1* (Ichimura et al., 1998, 2008) (Figure 1B), two biomarkers currently being assessed for clinical diagnosis of renal injury and repair (Bonventre and Yang, 2010; Haase-Fielitz et al., 2014). Upregulation of *Sox9* preceded activation of *Lcn2* and *Havcr1* consistent with *Sox9* engagement in the earliest phase of the injury response (Figure 1B). As with *Havcr1* and *Lcn2*, *Sox9* levels peaked around 24–48 hr post-injury (a 20-fold elevation in Sox9 levels in IRI versus sham surgery controls) paralleling the rise in serum creatinine. However, whereas creatinine levels were restored to baseline, *Sox9*, *Havcr1*, and *Lcn2* expression

expressed within nephron precursors though the relationship of $Sox9^+$ cells to future nephron structures and the potential actions of Sox9 in early nephrogenesis remain to be determined (Reginensi et al., 2011), The association of renal phenotypes as one component of the complex outcomes after loss of function of a single *SOX9* allele in man is consistent with a conserved renal action for *SOX9* in human kidney development (Foster et al., 1994; Wagner et al., 1994).

Here, we present evidence for *Sox9* engagement in PTEC repair after AKI. Lineage tracing demonstrates that the majority of cells that restore kidney function come from a $Sox9^+$ cell type. Interestingly, Sox9 activity highlights remaining regions of kidney damage after post-injury normalization of kidney function. Genetic analysis indicates Sox9 activity is critical for a normal repair process and developmental studies suggest Sox9 participates in normal nephrogenesis. Thus, Sox9 action provides a molecular link between formation and repair of the mammalian nephron.

remained elevated 28 days post-IRI indicative of an ongoing injury/repair response that may reflect an early stage in the AKI to CKD progression observed in the clinic (Figure 1B). The RNA-seq-based findings were independently corroborated by quantitative Fluidigm real-time PCR analysis on kidney samples (Figure 1C). Further, analysis of a unilateral ureteral obstruction (UUO) injury model highlighted a similar upregulation of *Sox9*, and the other injury-associated markers (Figure 1C). Thus, upregulation of *Sox9* is a general, early, and sustained transcriptional response to distinct initiators of kidney injury (Figure 1 C).

To determine which cells express SOX9 in the normal and injured kidney, we performed a detailed immunofluorescent analysis on kidney sections comparing SOX9 specific antibodies to a variety of antibody identifiers of key cell types in the mouse kidney. In the uninjured adult kidney, rare individual SOX9$^+$ cells were present in PTECs as visualized by co-labeling with Lotus tetragonolobus lectin (LTL) (0.05% of LTL$^+$ PTECs; Figure 1D). In addition, small clusters of cells were present in the calbindinD-28k positive (CALB1$^+$) distal tubule (DT) segment (4.1% of CALB1$^+$ DT; Figure 1E). No SOX9$^+$ cells were detected in the sodium potassium 2-chloride co-transporter positive (NKCC2/SLC12A1$^+$) thick ascending limb of the loop of Henle or in the Aquaporin2$^+$ collecting duct epithelium, the transit system for urine emerging from the nephron.

A marked increase in SOX9$^+$ cells was evident in PTECs 48 hr post-AKI (Figures 2A–C′). By this time, 10.6% ± 0.6% of LTL$^+$ PTECs were SOX9$^+$ (Figure 2C), and the majority of SOX9$^+$ cells were restricted to the PTEC (Figure 2C′; 92% ± 0.6% of SOX9$^+$ cells co-labeled as LTL$^+$; $p < 0.001$). A comparative analysis with de novo activation of the kidney injury response target HAVCR1 demonstrated SOX9$^+$ cells comprised a subset of the HAVCR1$^+$ population (Figures 2D–2F; 89% ± 6% of SOX9$^+$ cells were HAVCR1$^+$; $p < 0.001$).

In the normal adult kidney, PTECs are largely quiescent; injury is known to invoke a marked proliferative response within the HAVCR1 population 48 hr post-IRI (Witzgall et al., 1994) (Figures S1A and S1B). Ki67 labeling within injured PTECs indicates that a large fraction (~40%) of SOX9$^+$ cells were actively proliferating at this time (Figures 2G–2I). Similarly, in a UUO-induced AKI model, 10 days after obstruction, a significant increase in SOX9$^+$ cells occurred in a subset of HAVCR1-expressing population (98.4% ± 0.5% of SOX9$^+$ were HAVCR1$^+$, Figures S1C–S1E) with nearly half of the proliferating PTECs (LTL$^+$Ki67$^+$) expressing SOX9 (Figures S1F–S1H; LTL$^+$Ki67$^+$SOX9$^+$; 49% ± 0.6% cells). Similar to IRI-induced SOX9 activation, the vast majority of SOX9$^+$ was observed in nuclei of PTECs (Figures S1I; 97.4% ± 0.05% of SOX9% within the LTL$^+$ tubules) of which approximately 16% were actively proliferating at this time (Figure S1J). Thus, SOX9 demarcates a subset of proliferating, HAVCR1$^+$ PTECs in the setting of ischemic and obstructive AKI.

Transcriptional analysis in our severe AKI recovery model indicated that *Sox9* and *Havcr1* levels remain elevated 28 days post-IRI, 2 weeks after serum creatinine levels normalized (Figure 1B). Interestingly, we observed a population of SOX9$^+$/HAVCR1$^+$ co-labeled cells at this time (Figures 3A and 3D) with a higher concordance than the overlap 48 hr post-IRI (97% ± 0.5% of SOX9$^+$ cells were HACVR1$^+$; $p < 0.001$ at 28 days). Labeling was predominantly observed in dilated proximal tubules mosaic for LTL^{high}/SOX9$^-$ PTECs and zones of LTL^{low}/SOX9$^+$ cells without evident epithelial polarity typical of normal PTEC: an apical, LTL-enriched brush border (Figures 3B and 3E; 91% ± 1.9% of SOX9$^+$ cells were LTL$^+$). As at early stages, tubules retaining a reparative signature also demonstrated a high percentage of Ki67$^+$ proliferative cells predominantly within the SOX9$^+$ cell fraction of the proximal tubule (Figures 3C and 3F; 26% of SOX9$^+$ cells were Ki67$^+$). Together these data suggest that in tubules failing to resolve repair, SOX9$^+$ cells continue to mount a proliferative repair response that may have relevance to the enhanced likelihood of progression to CKD after AKI (see Discussion).

Sox9$^+$ Cells Are Major Contributors to Renal Tubule Repair

To determine whether *Sox9*$^+$ cells actively contribute to renal repair, we performed in vivo genetic fate mapping of *Sox9*$^+$ cells early on renal IRI. Adult mice expressing a tamoxifen (TM)-dependent form of Cre recombinase under control of the *Sox9* gene (*Sox9*$^{IRES\text{-}CreERT2/+}$; Furuyama et al., 2011) were crossed to a CRE-dependent td-Tomato reporter strain (*R26R*^{tdTomato}; hereafter referred to as *R26R*^{tdT}; (Madisen et al., 2010; Soriano, 1999). To confirm the reporter faithfully recapitulated, *Sox9* expression in the kidneys after IRI, we examined SOX9$^+$ and tdT$^+$ co-labeling 48 hr after IRI injury and TM injection in *Sox9*$^{IRES\text{-}CreERT2/+}$; *R26R*$^{tdT/+}$ mice. As expected, we observed a marked increase in SOX9$^+$ cells on IRI relative to sham surgery controls, and after injury, a subset of SOX9$^+$ cells displayed tdT fluorescence (tdT$^+$) on TM-mediated activation of the reporter; no reporter activity was observed on vehicle (corn oil) injection or in non-injected IRI controls (Figures 4A and 4B; data not shown). We did not find any evidence of "leaky" reporter in the kidneys. Furthermore, RNA-seq-based profiling of the tdT$^+$ cells in the kidney of sham animals confirmed 5-fold enrichment for Sox9 along with distal convoluted tubular markers, compared to the unlabeled population consistent with the immunofluorescence data and reporter activation studies (data not shown).

Next, we subjected *Sox9*$^{IRES\text{-}CreERT2/+}$:*R26R* $^{tdT/+}$ adult male mice to sham or renal IRI surgeries to obtain a fate map of early expressing *Sox9*$^+$ cells over a period of 4 weeks following injury. Initially, we administered three doses of tamoxifen over a 4-day period post-IRI (2 mg/animal/injection: 0, 48, and 96 hr post-injury) and examined kidneys 28 days after injury (Figures S2A–S2C).

In sham surgery control animals, rare scattered tdT$^+$ cells were restricted to LTL$^+$, Aquaporin-1$^+$ PTECs (Figures S2D and S2F), while clusters of tdT$^+$ cells were identified in CALB1$^+$ distal tubule segments (DT, Figure S2H) consistent with earlier SOX9 analysis in the uninjured adult kidney. No tdT$^+$ cells were observed in other tubular compartments of the nephron including NKCC2$^+$ cells of the thick ascending limb (TAL) of the loop of Henle (Figure S2J) or the aquaporin-2$^+$ collecting duct epithelium (CD, Figure S2L). In marked contrast, we observed extensive tdT labeling of the kidney after IRI (Figure S2C). The proximal tubule epithelium (LTL$^+$; Aquaporin1$^+$) was lined by tdT$^+$ cells (Figures S2E and S2G) and significant TdT$^+$ cells were detected in the loop of Henle (NKCC2; Figures S2J and S2K) and the CD (Aquaporin-2$^+$; Figures S2L and S2M); an enhanced tdT contribution was also observed in the DT (CALB1$^+$; Figures S2H and S2I).

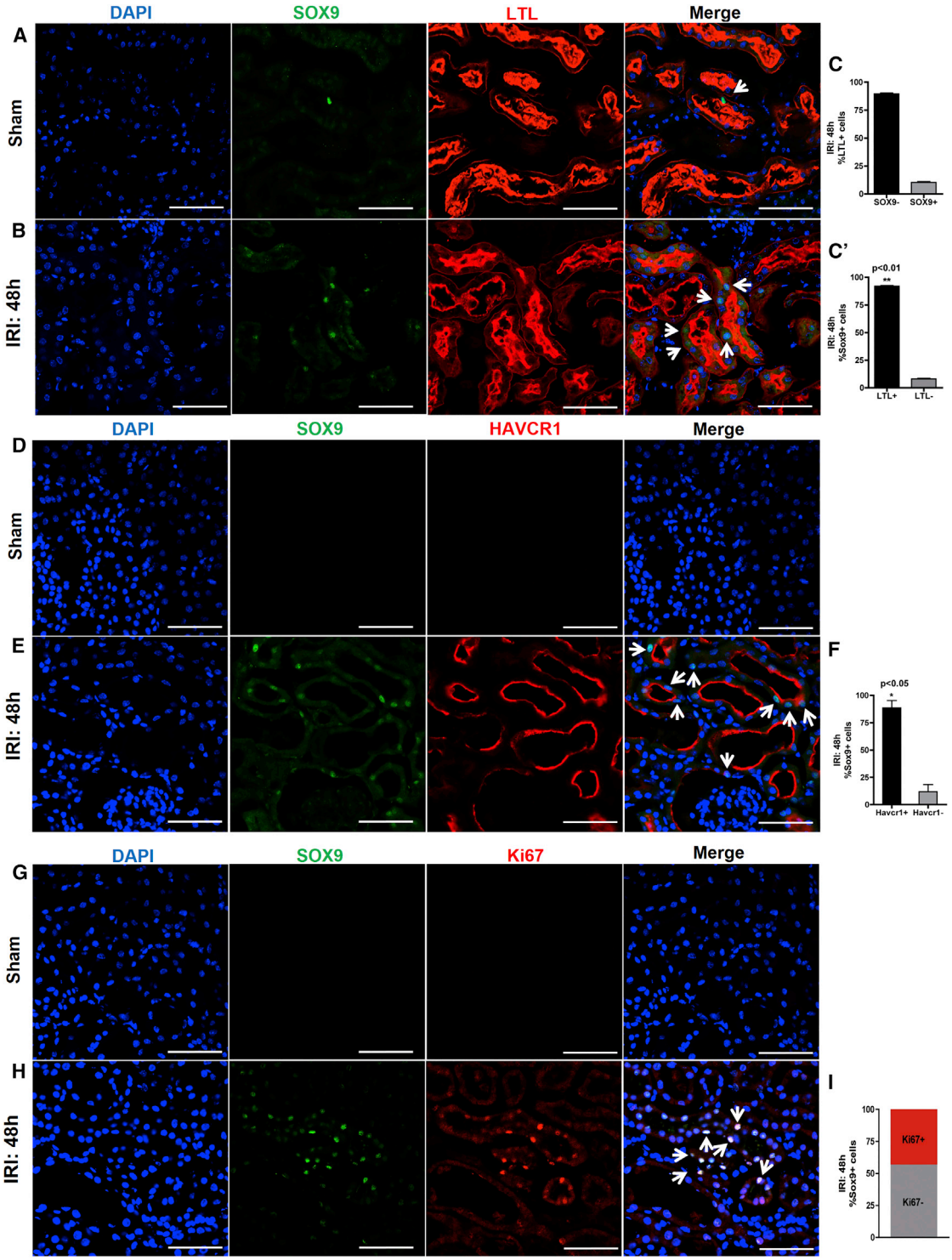

Figure 2. SOX9 Is Upregulated in the Injured, Proliferating Proximal Tubular Epithelial Cells 48 hr after Injury

(A and B) Immunoanalysis for SOX9 and LTL in kidneys 48 hr after sham (A) or renal IRI (B) surgery. Arrows highlight SOX9$^+$ cells.

(C and C′) Quantification of the percentage of LTL$^+$ proximal tubular cells expressing SOX9, and the percentage of SOX9$^+$ cells in LTL$^+$ proximal tubules (C′), 48 hr post-injury.

(D and E) Immunoanalysis for SOX9 and HAVCR1 in kidneys 48 hr after sham (D) or renal IRI (E).

(F) Quantification of the percentage of SOX9$^+$ cells in HAVCR1$^+$ injured tubules 48 hr post-injury.

(legend continued on next page)

Thus, IRI triggers a response that results in *Sox9*$^+$ cells contributing extensively to repair of the proximal tubule. Further, the great sensitivity of the CRE-system detects *Sox9* activation at levels not observed by direct antibody detection of Sox9 in other kidney epithelium. Thus, *Sox9* activation may be a broad, non-vascular epithelial response to stress sensing and damage where the degree of activation is linked to the severity of injury.

To obtain a better sense of the relationship between the earliest SOX9 activity and repair outcome, we performed a single, low-dose (1 mg/animal) TM administration immediately after IRI (Figure S3A). A 4-fold increase was observed in tdT$^+$ cells within 48 hr and a 20-fold increase by 28 days post-IRI (Figures 4C–4F). The marked increase between 2 and 28 days follows the onset of post-injury cell replication (Figures 4E and 4F). Proliferation of tdT$^+$ cells at 48 hr was confirmed by incorporation of EdU into nuclei undergoing DNA replication (Figures S3G and S3H).

Examination of tdT overlap with cell-type-specific markers showed that by 48 hr post-injury the fraction of tdT$^+$ cells was markedly increased in LTL$^+$ (Figures S3B, S3C, and S3E), Megalin$^+$, and ATP1A1$^+$ PTECs (Figures 4G, 4H, 4J, and 4K) relative to sham controls. This population of tdT$^+$ PTECs expanded further from 2 to 28 days post-IRI (Figures S3D and S3F; Figures 4I and 4L). Consistent with defective PT action, PTECs exhibited a loss of the normal basolateral membrane restriction of ATP1A1 (a critical membrane NaKATPase transporter) in tdT$^+$ cells 48 hr post-IRI; however, polarity was restored in tdT$^+$ cells 28 days post-injury (Figures 4J–4N). A normalization of apical cell polarity was also observed in apical megalin distribution (Figures 4G–4I). Together, these data indicate that *Sox9*$^+$ descendant cells proliferate and regenerate a functional proximal tubular epithelium after ischemic AKI.

Renal Repair by Resident SOX9$^+$ Cells and De Novo Activation of SOX9 in PTECs after IRI

To determine whether rare, resident *Sox9*$^+$ PTECs were responsible for the observed repair response, a multiday identical TM regimen was used to maximize pre-surgery labeling of the pre-existing *Sox9* population of both sham and animals that were subjected to renal IRI (2 mg/animal, three injections on 3 alternating days). After 2 weeks of washout to remove any TM, animals were subjected to sham or IRI surgery (Figure S4A). As expected, when the sham surgery procedure group was examined 28 days post-surgery, the vast majority of tdT$^+$/Megalin$^+$ PTECs were present as single cells in the uninjured cortices (Figures S4B and S4E; 94.8% ± 0.7%). The remainder consisted of contiguous two (2% ± 0.08%) or three cell clusters (0.2% ± 0.02%), and non-contiguous two cell groupings (3% ± 0.5%). None of the uninjured animals displayed more than three contiguous PTECs. In contrast, 4 weeks post-IRI, the proportion of single, tdT$^+$/Megalin$^+$ cells was significantly reduced (12% ± 0.7%, $p < 0.05$), while a substantial fraction (13.5%) comprised larger clusters with greater than ten contiguous cells (Figures S4C–S4E).

Together, these data suggest a limited expansion by resident *Sox9*$^+$ cells in the absence of injury over the 6-week course of the experiment but a marked expansion after IRI consistent with replication and repair by pre-existing *Sox9* cells. However, the overall extent of contribution of *Sox9*-descendant tdT$^+$ cells to the LTL$^+$ proximal tubules was markedly reduced (Figure S4F, 5.6% ± 1.0%) compared with the contribution after TM labeling of the Sox9$^+$ pool immediately after IRI (Figure S4F, 75.1% ± 2.2%, $p < 0.001$) suggesting an extensive contribution from PTECs that initiated de novo *Sox9* activation on injury. Consistent with this view, when all pre-existing *Sox9*$^+$ cells were tdT-labeled by a multi-day TM injection protocol (four consecutive injections of 3 mg/animal) (Figure S4G), the vast majority of LTL$^+$Sox9$^+$ cells were tdT- 48 hr post-IRI (90.5% ± 2.2%), thereby suggesting do novo activation of SOX9, in striking contrast to the LTL$^+$SOX9$^+$tdT$^+$ population (9.5% ± 3.1%), the resident SOX9$^+$ PTECs (Figures S4H and S4I). These data demonstrate that PT repair is realized predominantly by PTECs that undergo de novo activation of *Sox9* after AKI rather than an expansion of a pre-existing, intra-tubular resident *Sox9*$^+$ PTEC population.

Sox9 Is Required for Normal Proximal Tubular Repair after Ischemic AKI

Next, we sought to examine whether *Sox9* activity is required for PTEC repair after IRI. To this end, we made use of an *Slc34a1*$^{CreERT2/+}$ strain (Kusaba et al., 2014) to drive robust TM-dependent CRE activity within S1 and S2 segments of the PT. Though these cortical PT segments were less severely affected than the S3 outer medullary segment after IRI (Bonventre and Yang, 2011), a substantial contribution of tdT$^+$ descendants of *Sox9*$^+$ cells was observed in both S1 and S2 segments. Injection of four doses of TM (3 mg/mouse/injection) on alternate days gave widespread reporter activation in 98.8% of cells within the cortical LTL+ PT (Figures S5A–S5D). Analysis of SOX9$^+$ cells post-IRI demonstrated an expected overlap with the *Slc34a1*$^{CreERT2/+}$ labeled tdT$^+$ PTECs (Figure S5E).

The injury-repair process was compared in adult kidneys of *Slc34a1*$^{CreERT2/+}$*:Sox9*$^{fl/+}$ mice retaining a single active *Sox9* allele in the S1 and S2 PT segment post-TM injection with that of *Slc34a1*$^{CreERT2/+}$; *Sox9*$^{fl/fl}$ mice where all *Sox9* activity was removed from S1 and S2 segments, verified by SOX9 immunostaining (Figure 5A; Figures S5F and S5G). Whereas creatinine levels approached baseline (0.2 ± 0.04 mg/dl, Figure 5B) 5 days post-IRI in control mice retaining Sox9 activity in S1/S2 segments (*Slc34a1*$^{CreERT2/+}$*:Sox9*$^{fl/+}$), S1-S2-specific Sox9-deficient mice (*Slc34a1*$^{CreERT2/+}$*:Sox9*$^{fl/fl}$) displayed significantly elevated serum creatinine levels (0.56 ± 0.28 mg/dl, $p < 0.01$, Figure 5B). However, by 28 days post-IRI, serum creatinine levels were normalized in both groups (Figure 5B). Thus, loss of SOX9 appears to slow but not prevent physiological renal repair by this functional metric.

A blinded histological scoring of tubular epithelial injury in the cortical S1 and S2 segments post-IRI revealed an enhanced

(G and H) Immunoanalysis for SOX9 and Ki67 in kidneys 48 hr after sham (G) or renal IRI (H).

(I) Quantification of percentage of SOX9$^+$ cells coexpressing Ki67 after injury.

White arrows (E and H) point to the SOX9-expressing cells. Data shown in (C) and (F) are represented as mean ± SEM (*$p < 0.05$, **$p < 0.01$, n = 3 mice/group). DAPI demarcates nuclei. Scale bar, 100 μm. See also Figure S1.

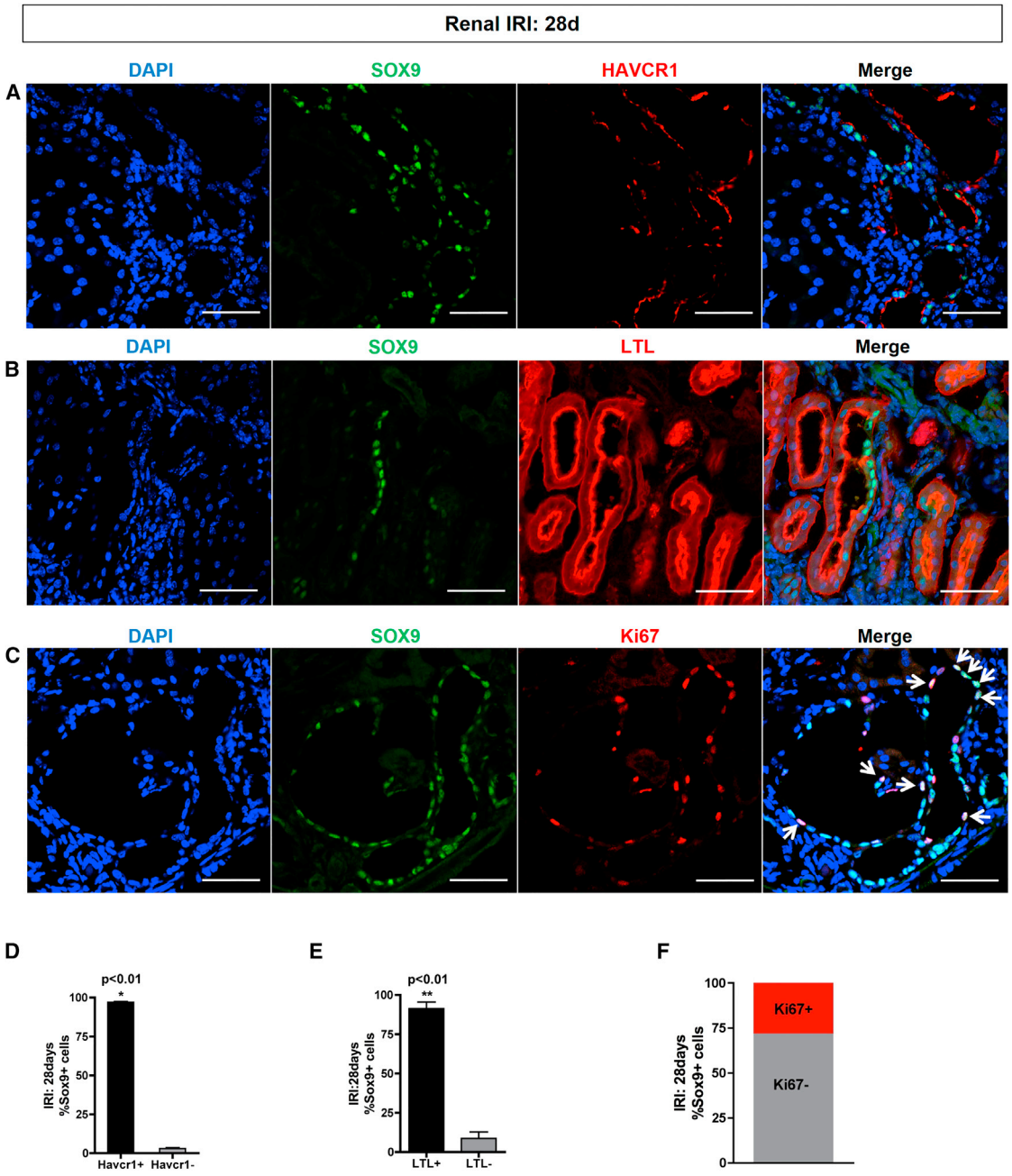

Figure 3. Persistent Regional SOX9 Activity in Proximal Epithelial Tubules Displaying Ongoing Proliferative Repair Responses 28 Days Post-IRI

(A) Immunoanalysis for SOX9 and HAVCR1 28 days post-IRI.

(B) Immunoanalysis for SOX9 and LTL 28 days post-IRI.

(C) Immunoanalysis for SOX9 and Ki67 28 days post-IRI. White arrows highlight SOX9$^+$ cells.

(D) Quantification of percentage of SOX9$^+$ cells in HAVCR1$^+$ tubules 28 days post-IRI.

(E) Quantification of percentage of SOX9$^+$ cells in LTL$^+$ proximal tubules 28 days post-IRI.

(F) Quantification of percentage of SOX9$^+$ and Ki67$^+$ cells 28 days post-IRI

Data shown in (D) and (E) are represented as mean ± SEM (**$p < 0.01$, $n = 3$ mice/group). DAPI demarcates nuclei. Scale bar, 100 μm.

initial injury (5 days) and more dramatic tubular epithelial damage response remaining 28 days post-IRI in the cortical S1 and S2 segments of Sox9-deficient mice (Figures 5C–5J); HAVCR1 immunostaining analysis provided additional evidence for comprised repair in Sox9-deficient PTECs (Figures S5H and S5I). When assayed by qPCR for a series of fibrotic indicators, the

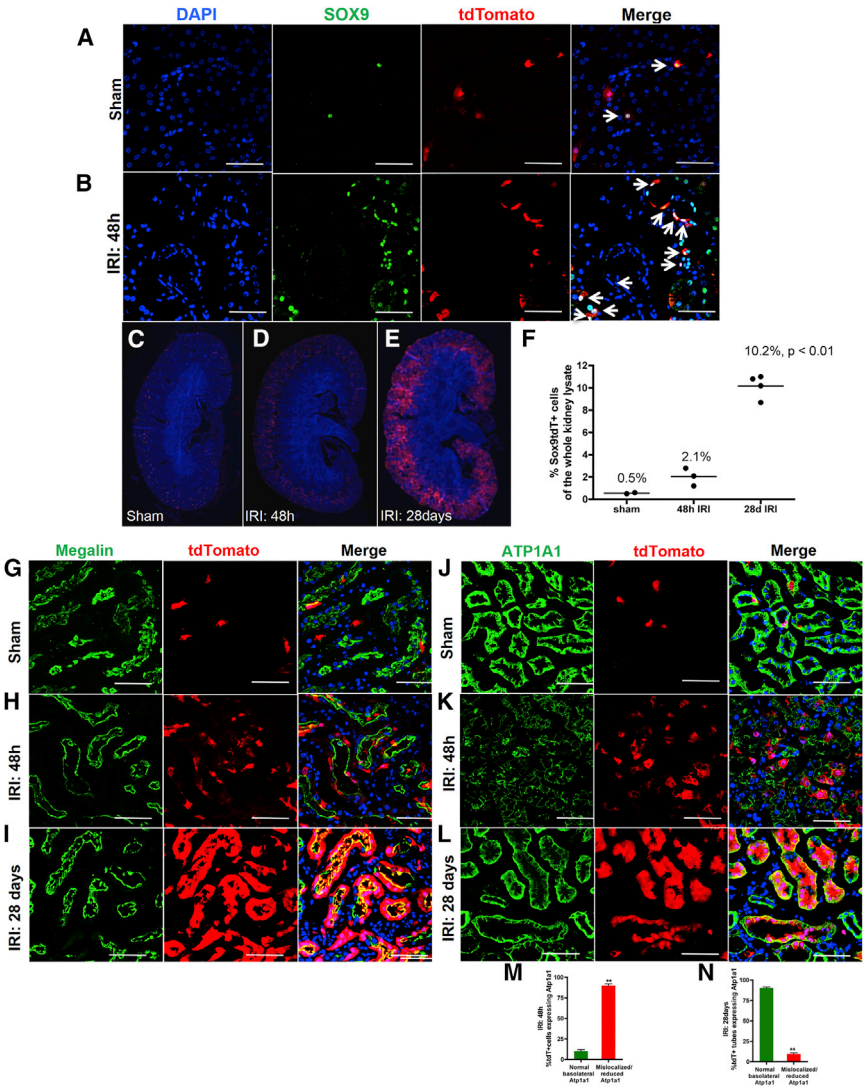

Figure 4. Proliferation and Repair of Proximal Tubule Epithelium by SOX9$^+$ Cells Present Early on IRI

(A and B) Immunoanalysis for SOX9$^+$ cells demonstrates co-localization with SOX9-CREERT2-activated tdTomato fluorescence (tdT$^+$) in sham surgery (A) and IRI (B) kidneys 48 hr post-TM injection and surgery. Arrowheads highlight SOX9$^+$/tdTomato$^+$ co-labeled cells.

(C–E) Representative images of tdT$^+$ cells in whole scanned kidneys harvested from mice that underwent sham surgery (C), or IRI: 48 hr post-IRI (D), 28 days (E) post-IRI. Scale bar, 1,000 μm.

(F) Fluorescence-activated cell sorting (FACS) quantification of tdT$^+$ cells at baseline (sham animals), 48 hr, and 28 days post-IRI (sham, n = 3; IRI: 48 hr and 28 days, n = 4 mice/group).

(G–L) Immunoanalysis for megalin (G–I) and ATP1A1 (NaKATPase; J–L) in sham surgery (G and J), and IRI kidneys: 48 hr (H and K) and 28 days (I and L) post-IRI.

(M) Quantification of the percentage of tdT$^+$ cells with normal or reduced and/or mislocalized ATP1A1 (NaKATPase, normally polarized to basolateral membrane surfaces) 48 hr post-IRI.

(N) Quantification of the percentage of tdT$^+$ *Sox9*-descendent cells normal and reduced and/or mislocalized ATP1A1 28 days post-IRI.

Data in (M) and (N) are represented as mean ± SEM (**p < 0.01, n = 3 mice/group). DAPI demarcates nuclei. Scale bar, 100 μm. See also Figures S2–S4.

cortices of S1-S2-specific Sox9-deficient mice showed a markedly enhanced signature of renal fibrosis (Figures 5K–5N). Thus, *Sox9* activity is required within PTECs for a normal repair process.

Activation of the Wnt-β-catenin pathway has recently been linked to PTEC repair in ischemic AKI (Rinkevich et al., 2014). To examine the relationship between canonical Wnt signaling and Sox9-driven tubular epithelial repair responses, we subjected *TCF/Lef:H2B-GFP* mice, a Wnt/β-catenin signaling reporter mouse strain (Ferrer-Vaquer et al., 2010) to sham or renal IRI surgery. In the sham kidneys, 16.2% ± 2.3% of the megalin$^+$ PTECs displayed a GFP^{low} (GFP^{low+}) and 6.1% ± 2.3% a GFP^{high} signal (GFP^{high+}) (Figures S6A, S6C, and S6E), a much larger fraction than the SOX9$^+$ PTECs (0.05% of LTL$^+$ PTECs). No SOX9$^+$ cell co-localized with the GFP^{low+} or GFP^{high+} cells in uninjured kidneys. Forty-eight hours post-IRI, a significant increase was observed in both GFP^{low} (28.2% ± 4.2%) and GFP^{high} (28% ± 3.2%) populations of megalin$^+$ PTECs consistent with broad canonical Wnt/β-catenin pathway signaling in PTECs after IRI (Figures S6B, S6D, and S6E). Though a substantial proportion of SOX9$^+$LTL$^+$ cells co-localized with the GFP reporter (26.4% ± 4.5%; Figures S6D, S6D′, S6F, and S6G), the overlap of SOX9$^+$ and GFP$^+$ cells was not significantly higher than that expected by chance at this time point (binomial p value = 0.9). Thus, the data suggest that the SOX9$^+$ cells constitute a distinct population with no significant enrichment for engagement of the Wnt/ β-catenin pathway in its epithelial reparative response 48 hr after ischemic AKI.

Sox9 Is Required for Normal Development of Proximal Tubule Regions

To determine whether *Sox9* combines a role in PTEC repair with development of the PT, we examined SOX9 in the developing mouse kidney. In the embryonic kidney 17.5 days post-fertilization (e17.5), SOX9 was present in both the tips of the branching ureteric tree and within distal regions of the S-shaped nephron precursors (Figures S7A–S7C). By post-natal stage 4 (P4), branching ceases and a final wave of nephrogenesis takes place so that SOX9 was only detected in the developing nephron population (Figures S7D and S7E).

To fate map Sox9$^+$ cell descendants during kidney development, tamoxifen was injected into pregnant *Sox9$^{IRES\text{-}CreERT2/+}$:R26R$^{tdT/+}$* dams (single 2-mg dose) at e16.5 and tDT$^+$/SOX9$^+$ cells identified at e17.5 (Figure 6A). As expected, we observed

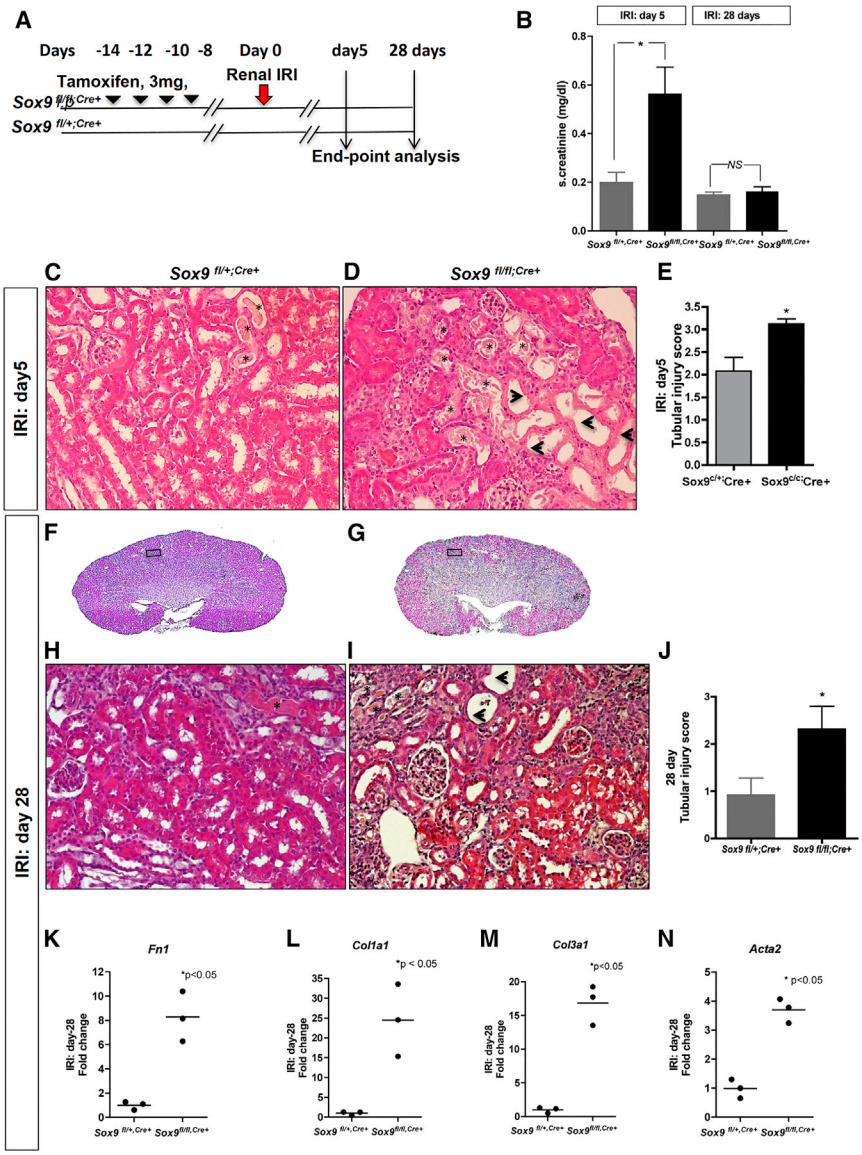

Figure 5. Tamoxifen-CRE-Dependent *Sox9* Removal from S1 and S2 Proximal Tubule Segments Impairs Renal Recovery Post-IRI

(A) Experimental outline of SOX9 removal before IRI. Control (*Slc34a1*$^{CreERT2/+}$:*Sox9*$^{fl/+}$) and experimental groups (*Slc34a1*$^{CreERT2/+}$:*Sox9*$^{fl/fl}$) were administered tamoxifen pre-IRI (3 mg for four doses, alternate days, i.p.), and subjected to IRI 1 week after the final TM injection.

(B) Serum creatinine measurements 5 and 28 days post-IRI (*p < 0.05, *Slc34a1*$^{CreERT2/+}$:*Sox9*$^{fl/fl}$ versus *Slc34a1*$^{CreERT2/+}$:*Sox9*$^{fl/+}$; NS, non-significant; n = 6 animals/group).

(C and D) Representative images of H&E-stained cortical kidney sections. Asterisks indicate casts in renal tubules and arrowheads highlight denuded regions of epithelia.

(E) Quantitative scores of acute tubular injury 5 days post-IRI (*p < 0.05, *Slc34a1*$^{CreERT2/+}$:*Sox9*$^{fl/fl}$ versus *Slc34a1*$^{CreERT2/+}$:*Sox9*$^{fl/+}$; n = 5 animals/group).

(F and G) Representative images of H&E-stained whole kidney sections 28 days post-sham (F) or IRI (G) surgery.

(H and I) Representative images of H&E-stained cortical kidney sections. Asterisks indicate tubules retaining casts, and arrowheads highlight atrophied, dilated tubules.

(J) Quantitative scores of tubular injury 28 days post-IRI (*p < 0.05, *Slc34a1*$^{CreERT2/+}$:*Sox9*$^{fl/fl}$ versus *Slc34a1*$^{CreERT2/+}$:*Sox9*$^{fl/+}$; n = 5 animals/group).

(K–N) qPCR analysis of increased fibrosis in the kidney cortices after Sox9 removal. Fibrosis was assessed comparing genes associated with renal fibrosis, *Fn1* (K), *Col1a1* (L), *Col3a1* (M), and *Acta2* (N) between *Slc34a1*$^{CreERT2/+}$:*Sox9*$^{fl/fl}$ versus *Slc34a1*$^{CreERT2/+}$:*Sox9*$^{fl/+}$ mice 28 days after injury (*p < 0.05; n = 3 mice/group).

Data in (B), (E), and (J) are represented as mean ± SEM. See also Figure S5. Scale bar, 200 μm. See also Figures S5 and S6.

an overlap of tDT$^+$ cells in the ureteric tips with some additional extension of tDT$^+$ cells into adjacent stalk regions indicative of commitment of a subset of cells within the Sox9$^+$ tip progenitor pool. In the developing nephron, labeling was observed in distal components of the S-shaped body to the nephron junction with the ureteric epithelium (Figures 6B–6E). When chased for 6 weeks into the adult kidney, tdT$^+$ cells localized to Aquaporin-2$^+$ collecting duct epithelium extending into the renal pelvis (Figure 6F), and most segments of the nephron but not the glomerular region (Figures 6G–6I). Extensive nephron labeling was also evident from imaging intact micro-dissected nephrons (Figure S6G). These data indicate that descendants of a *Sox9*$^+$ cell contribute to most non-vascular epithelium within the normal kidney.

These results raise the possibility that *Sox9* may play a normal role in nephron development in addition to nephron repair. *Sox9* and Sox8 have been shown to regulate branching growth of the ureteric network where the two genes are co-expressed (Reginensi et al., 2011). The nephron primordium only expresses *Sox9*, consequently *Pax2Cre*-driven genetic inactivation in a Sox8/9 conditional mutant model removes Sox9 activity in the nephron compartment in addition to removing *Sox8* and *Sox9* activity were each gene is co-expressed and co-active at ureteric branch tips (Reginensi et al., 2011). Interestingly, kidneys from mutant mice showed an absence of *Slc5a*$^+$ *and Slc5a2*$^+$ proximal tubule (Figures 7E–7H) and *Slc12a3*$^+$ distal tubule (Figures 7I and 7J) segments, while the *Slc12a1*$^+$ thick ascending limb of the loop of Henle was less severely affected (Figures 7K and 7L). Together, the findings are consistent with Sox9 playing a role in normal nephron development and renal repair.

DISCUSSION

We have identified *Sox9* activation as a central component of the early damage and repair response of injured renal tubule cells.

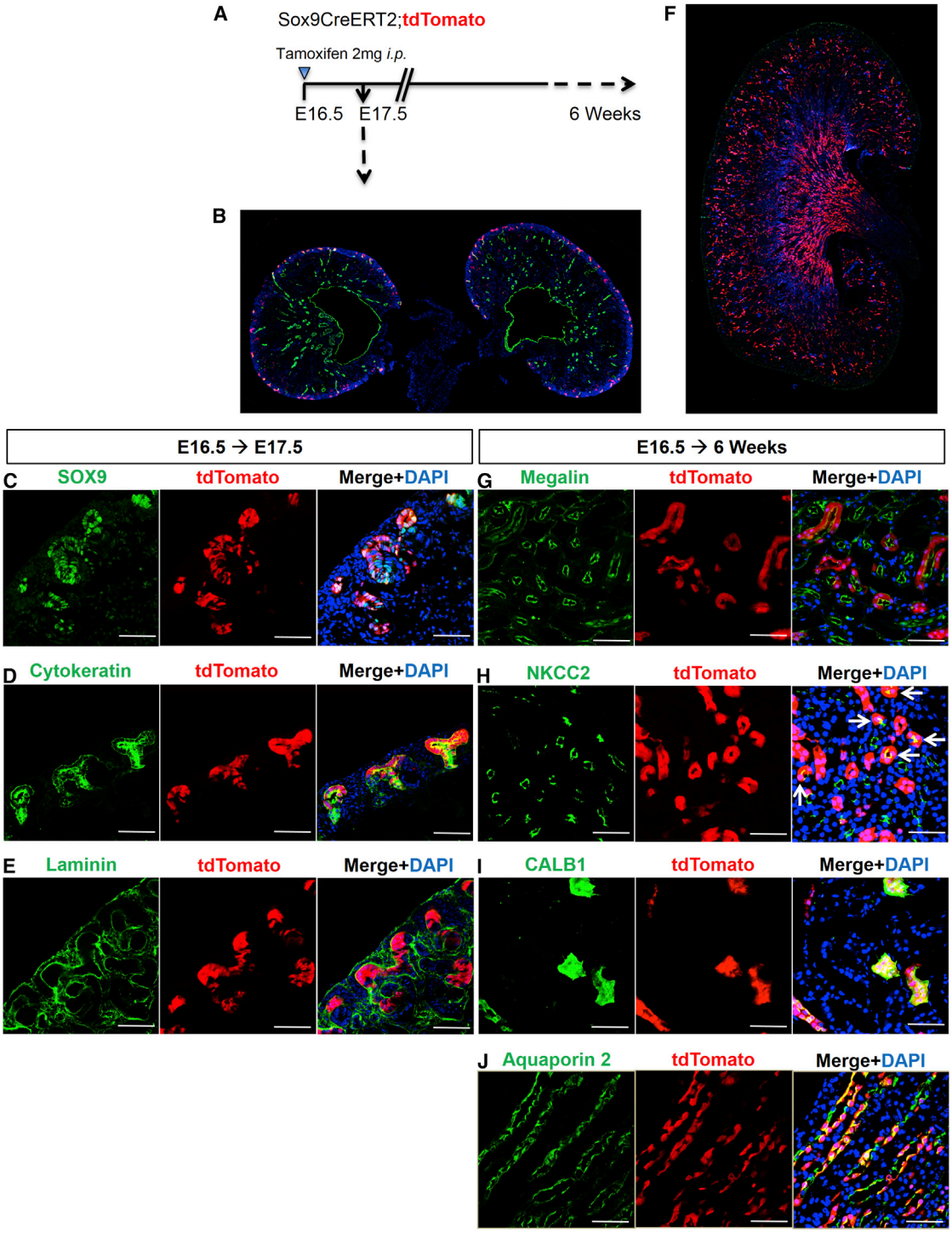

Figure 6. Fate Mapping of *Sox9*$^+$ Cell Descendants Shows Extensive Contribution to the Ureteric and Nephron Epithelia

(A) Experimental outline of fate mapping of the *Sox9*$^+$ population in *Sox9*$^{IRES\text{-}CreERT2/+}$*: R26R* $^{tdT/+}$ embryos. A single tamoxifen (2 mg i.p.) dose was injected at 16.5 dpc. Kidneys were harvested at 17.5 dpc and at 6 weeks postnatally.

(B) Immunoanalysis for tdT and cytokeratin (green, ureteric epithelium). Representative images of whole kidneys scanned at E17.5. Scale bar, 100 μm.

(C) Immunoanalysis of SOX9$^+$ and tDT$^+$ cells in E17.5 kidneys.

(D and E) Immunoanalysis for cytokeratin (D, ureteric epithelium) and laminin, (E, broad basement membrane marker) and tdT in E17.5 kidney.

(legend continued on next page)

SOX9$^+$ cells re-enter mitosis and contribute extensively to restoration of the proximal tubule. Activation of *Sox9* is also observed in other non-vascular tubular components less susceptible to IRI using sensitive recombination-mediated reporters suggesting that *Sox9* may be targeted by a broad organ wide stress response with maximal, immunodetectable levels in the most metabolically active and stress-sensitive cells of the proximal tubule. Analysis of a UUO kidney injury model suggests that activation of *Sox9* is a general response to tubular injury.

Genetic studies focused on S1 and S2 segments of the proximal tubule indicate that SOX9 is important in the kidney repair process; SOX9 removal from these cells delayed the normalization of kidney function and increased the residual kidney damage signature. Interestingly, several weeks after restoration of kidney function, foci of undifferentiated SOX9$^+$ cells remained within the proximal tubule. Co-expression of the injury reporter HAVCR1$^+$, and the absence of molecular indicators of normal PT cell function and polarity within this population, suggests that ongoing SOX9 activity highlights tubular domains where epithelial function has not been restored, and an unresolved repair process remains active. Clinical studies have highlighted a link between an episode of AKI and the long-term progression to CKD (Chawla et al., 2014; Coca et al., 2012). In this, the predominant focus has been on pathological inflammatory responses in the kidney seeded by initial fibrotic interstitial scarring within the pericyte population that is first evident within a few days of AKI (Humphreys et al., 2010; Kramann and Humphreys, 2014). Our findings suggest that damaged kidney tubules locked into a repair response that fails to terminate may represent an additional mechanism triggering long-term maladaptive responses that ultimately lead to the loss of kidney function.

In development, SOX9 is present in the early developing nephron and at the tips of the branching ureteric network where the progenitors for the entire ureteric network reside (Reginensi et al., 2011; Shakya et al., 2005). Our cell-fate studies demonstrate that much of the non-vascular epithelium within the kidney is derived from a *Sox9*$^+$ cell type. Thus, there is a close relationship between the shared lineage of mature tubular epithelial cells in the adult kidney from earlier SOX9$^+$ renal progenitor populations, and kidney epithelia activating *Sox9* on AKI.

The repair process does not broadly recapitulate developmental stages of renal tubule specification and patterning though there is some evidence for reactivation of specific regulatory components (Abbate et al., 1999; Imgrund et al., 1999; Lindoso et al., 2009; Terada et al., 2003; Villanueva et al., 2006). Our analysis of *Sox8* and *Sox9* compound mutants that lack *Sox9* activity within forming nephrons revealed a marked deficiency of proximal and distal nephron segments consistent with a role of Sox9 within the developmental program. We also observe very rare SOX9$^+$ cells (less than 0.1% of all mature cell types) that co-express mature tubular markers in proximal tubule segments of the uninjured adult kidney, and clusters of cells within distal tubule segments. These findings suggest *Sox9* may play a limited role within the adult nephron, particularly within distal tubule cell types. Whether there are common molecular actions for Sox9 in development and adult renal tubule function, maintenance, and repair remains to be determined. Given the action of Sox9 (like other Sox family members) as a pioneer transcription factor in many cellular programming events, direct analysis of Sox9 DNA-target interactions, though technically challenging, is likely to provide an important insight into the regulatory mechanisms at play.

SOX9$^+$ Cells and Cellular Mediators of Renal Tubule Repair

Genetic lineage tracing studies have shown that intrinsic tubular epithelial cells proliferate and repair the injured epithelium in the mouse kidney (Berger and Moeller, 2014; Humphreys et al., 2008; Kusaba et al., 2014). Our data lend additional support to this model. SOX9 was clearly present with mature PT cells as determined by co-labeling with LTL, aquaporin-1, megalin, and ATP1A1. Further, pulse-chase cell-fate tracing of the earliest cells activating *Sox9* in response to IRI through a single TM injection at the time of IRI predominantly labeled intratubular epithelial cells that expanded significantly to effect repair over the 28 day post-injury study period.

Whether PT repair is directed by a specific cell type within the epithelium or represents a broad response open to any PT cell surviving injury and activating an appropriate repair pathway remains contentious. Studies with an NFATc1-CRE mouse strain have linked an NFATc1$^+$ cell type to tubular repair (Langworthy et al., 2009). Others have invoked a rare CD133$^+$CD24$^+$ cell retaining an uncommitted early nephron potential as the cellular mediator of human and mouse PT repair (Angelotti et al., 2012; Lazzeri et al., 2007). However rigorous cell-fate tracing, the only definitive approach to relate cell type to specific injury is clearly problematic for human kidney studies.

Strong evidence in favor of repair by mature cortical PTECs comes from tracing descendants of *Slc34a1*$^+$ cells in the S1 and S2 segments of the PT (Kusaba et al., 2014). Further, clonal analysis comparing descendants of individual, randomly labeled *Slc34a1*$^+$ cells found no evidence for dramatically variable clone size among the clonal populations supporting a model wherein all cells have similar regenerative capability (Kusaba et al., 2014). Similar conclusions have been drawn from a rhabdomyolysis-induced AKI model were cell labeling is not restricted to the PT compartment of the kidney (Rinkevich et al., 2014).

Though we observe rare SOX9$^+$ PTECs in the uninjured adult kidney, pre- and post-injury pulse-chase labeling and cell-fate tracking of the descendants of SOX9$^+$ cells suggest these cells have a minor contribution overall to the repair process. As one example, significant proliferative activity is first evident 48–72 post-IRI, but by 48 hr there is already a marked increase in SOX9$^+$ cells within damaged PT segments that cannot be accounted for by expansion of a rare resident Sox9$^+$ cell type. The major contribution must come from de novo activation of

(F) Representative image of the tDT in whole scanned 6-week old kidneys harvested after labeling with single dose of tamoxifen (2 mg, i.p.) at E16.5.
(G–J) Detailed analysis of tdT$^+$ kidney labeled as in (F). Immunoanalysis for megalin (G, proximal tubular epithelium), NKCC2 (H, thick ascending limb of loop of Henle), CALB1 (I, calbindin-28 dk, distal convoluted tubule), and aquaporin2 (J, collecting duct).
Representative images taken from n = 3 mice/group. Scale bar, 100 μm. See also Figure S7.

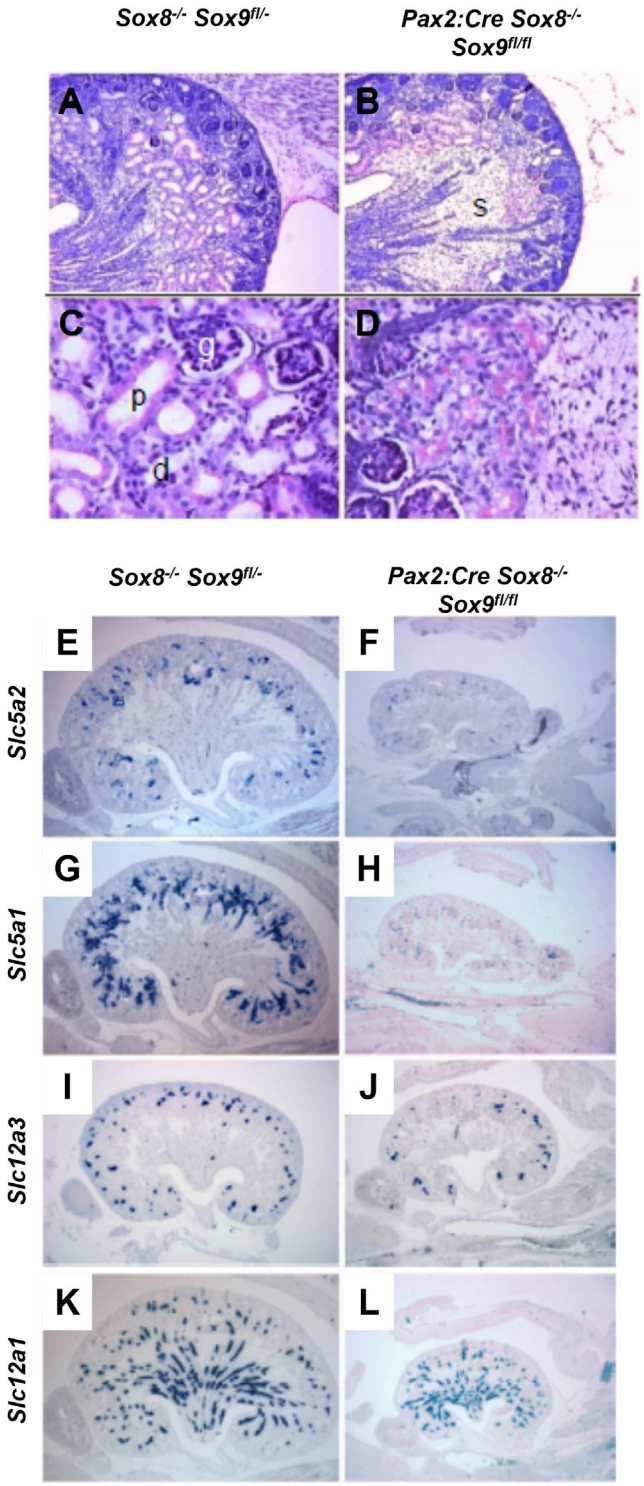

Figure 7. *Sox9* Removal from the Mouse Kidney Results in a Marked Reduction of Nephron Components

(A–D) PAS staining of E18.5 kidneys from wild-type and *Pax2:Cre;Sox9*$^{fl/fl}$; *Sox8*$^{-/-}$ mutant animals. Glomerulus (g), proximal tubule (p), distal tubule (d). Scale bar, 200 μm.

(E–L) RNA in situ hybridization for *Slc5a2* (E and F) and *Slc5a1* (G and H) (sodium glucose linked transporter-2 and -1, respectively; proximal convoluted tubule specific markers), *Slc12a3* (I and J) (thiazide-sensitive sodium chloride cotransporter: distal convoluted tubule specific marker), and *Slc12a1* (K and L) (sodium potassium 2 chloride cotransporter: thick ascending limb of loop of Henle specific marker). Scale bar, 100 μm.

Sox9 in surviving differentiated PTECs. Importantly, this does not rule out a role for a rare SOX9^{+} PTEC in renal tubule maintenance under normal physiological conditions; additional studies will be required to examine this population in more detail.

Recent experiments examining canonical Wnt-pathway reporters have suggested activation of canonical Wnt-signaling accompanies PTEC repair (Rinkevich et al., 2014). In the uninjured adult kidney, we observe a substantial fraction of PTECs have activated a canonical Wnt reporter (approximately 30%). Given the nature of the reporter, which utilizes a GFP-tagged histone as readout of pathway activation, we cannot determine whether signaling reflects ongoing or historical signaling, and if historical when relative to the time of analysis. However, it is clear there is no significant overlap in Wnt-response in normal PTECs and rare SOX9^{+} cell types. A significant overlap is observed in cells displaying Wnt-reporter expression post-injury and SOX9^{+} cells. The fraction of both cell types within the population of PT cells increases post-injury, more dramatically for SOX9 (SOX9^{+} cells and TCF/Lef1:H2B-eGFP^{+} cells increased by 20- and 5-fold, respectively, 48 hr after injury) as a result of broad, injury invoked de novo activation. However, there are clearly many cells that are Sox9^{+} and Wnt reporter negative (73.6% ± 2.4%) and Wnt reporter positive and Sox9^{-} (92.1% ± 6.5%), and statistical analysis indicates there is no significant co-association between the two cellular populations. Thus, there is no clear-cut relationship between Wnt pathway induction and *Sox9* activity that can be discerned in the current analysis of renal repair.

Sox9 Action in Tissue Specification, Homeostasis, and Repair

In development, *Sox9*, like other Sox-family members, maintains stem cell/progenitor states and promotes the differentiation of mature cell types depending on the organ system, timing, and tissue type (Kamachi and Kondoh, 2013; Sarkar and Hochedlinger, 2013). *Sox9* maintains the stem/progenitor cell state of hair follicles (Nowak et al., 2008), multi-potent retinal progenitor cells (Poché et al., 2008), neural stem cells (Cheung and Briscoe, 2003), and *Sox9* is upregulated in mammary stem cells (Guo et al., 2012). *Sox9* also plays a pivotal role in the programming of embryonic liver and pancreas progenitors (Kawaguchi, 2013), elaboration of all skeletal structures (Wright et al., 1995), and gonadal sex determination (Kent et al., 1996), and *Sox9* activity marks pituitary progenitors of endocrine lineages (Rizzoti et al., 2013).

Interestingly, SOX9^{+} cell types have been linked to epithelial-based repair in the pancreas and liver after injury suggesting possible parallels with the injury responses in the kidney. SOX9 is upregulated in the urothelium after varied insults including exposure to carcinogen and hydrogen peroxide (Ling et al., 2011). These studies have implicated epidermal growth factor receptor/extracellular signal-regulated kinases1/2 (EGFR/ERK1/2) signaling in *Sox9* induction. As ERK1/2 signaling is rapidly

activated after renal IRI (Kumar et al., 2009), this pathway is one candidate for mediating Sox9 activation. Hypoxia-mediated induction may represent another. In chondrocyte development, hypoxia-inducible factor-1 alpha (*Hif1a*) directly binds to the *Sox9* promoter regulating *Sox9* expression (Zhang et al., 2011). Sox9 is also known to regulate its own expression in chondrocytes and Sertoli cells of the testis (Mead et al., 2013). Thus, persistent *Sox9* expression in unresolved repair could reflect ongoing *Sox9* induction by Sox9-independent regulatory processes, or the absence of inhibitory factors that normally terminate SOX9's auto regulatory action on successful repair of PT epithelium.

In vertebrates, the dedifferentiation of quiescent differentiated cells into a replicating progenitor or progenitor-like cell state has been linked to the repair of epithelial airways (Tata et al., 2013). Here, there may be parallels here with the AKI model. On AKI, a serious life-threatening event, the drive is to rapidly replace up to 80% of PTECs to ensure the individual's survival. The PT is a complex, highly organized structure with distinct regional foci of transporter and channel proteins mediating its essential physiological actions. The rapid reprogramming by stress responses of surviving, quiescent differentiated cells to a proliferative state, while simultaneously preserving a cell's positional identity within the nephron to enable the reformation of appropriate, regionally restricted differentiated cell types, would be an effective means to this end. Interestingly, clonal studies of renal repair have highlighted the regionally restricted differentiation capability of repairing cells consistent with this view (Rinkevich et al., 2014).

In summary, our data provide evidence for *Sox9* activation as an early transcriptional response to renal injury. Further, *Sox9* likely acts as a broad facilitator of epithelial repair. *Sox9* co-opted organ repair contrasts with stem-cell-based models of repair identified in many organ systems. As such, a *Sox9*-directed mechanism may represent an expedient, alternative repair process designed to rapidly recruit any surviving mature cell type post-injury into a transient reparative state.

EXPERIMENTAL PROCEDURES

See Supplemental Experimental Procedures for an extended and detailed description of the materials and methods used.

Mice and Injury Models

Sox9$^{IRES\text{-}CreERT2/+}$ (Furuyama et al., 2011), *R26R*$^{tdTomato/tdTomato}$ (JAX stock number 007909), *Slc34a1*$^{CreERT2/+}$ mice (Kusaba et al., 2014), *TCF/Lef:H2B-GFP* mice (JAX stock number 013752), *Sox9*$^{fl/fl}$ (JAX stock number 013106), and *Pax2Cre:Sox8/9* double-knockout mutants mice were described previously (Reginensi et al., 2011). Renal ischemia reperfusion injury and unilateral ureteral obstruction models followed published injury-modeling procedures (Fabian et al., 2012). Adult (10–12 weeks, 25–28 g) male mice were employed for all adult experimental analysis. Standard analysis used C57BL/6 inbred strains. All surgical procedures, and all mouse handling and husbandry were performed according to guidelines issued by the Institutional Animal Care and Use Committees (IACUC) at each institution.

For lineage tracing in the embryonic kidney, noon on the day of vaginal plug detection was considered embryonic day 0.5 (E0.5). For induction of CreERT2 protein, mice were injected with tamoxifen (Sigma, #T5648) dissolved in corn oil (Sigma, #C8267) via an intra-peritoneal (i.p.) route. The dosing schedule, frequency, and timing of the administration are documented in relation to the experiment in the results section.

Immunofluorescence, Histology, In Situ Hybridization, Microscopy, and Imaging

Kidneys were harvested and fixed by intra-cardiac perfusion with 4% paraformaldehyde. Immunofluorescence was performed on 6-μm cryosections using primary and secondary antibodies described in the Supplemental Information. Images were acquired using either a confocal microscope (Carl Zeiss 780 LSM), or slide scanner (Zeiss Axioscan.Z1). For conventional histology, H&E or periodic acid-Schiff (PAS) staining was performed according to the routine histology protocols on 5-μm-thick paraffin sections. Semiquantitative analysis of tubular morphology was performed in a blinded fashion as described in the Supplemental Information. Images were acquired on a slide scanner (Zeiss Axioscan.Z1) and upright Nikon Eclipse 90i microscope. In situ hybridization and histology of embryonic kidneys is detailed in the Supplemental Information.

Quantifying Transcript Levels in Kidney Cell Types

The use of RNA-seq and Fluidigm PCR to assess transcription in whole kidneys or kidney subsets of kidney cells are described in the Supplemental Information. This includes details on kidney digestion and FACS of cell types.

Statistical Analysis

All values are reported as mean ± SEM. Statistical significance was calculated by the unpaired t test for unpaired observations. All statistical analysis was performed using GraphPad Prism v.4.03 (GraphPad Software). A binomial p value significance test was used to examine association between SOX9 and GFP expression. p values of 0.05 or less were considered significant. All t tests used two-sided t test analysis.

SUPPLEMENTAL INFORMATION

Supplemental Information includes Supplemental Experimental Procedures and seven figures and can be found with this article online at http://dx.doi.org/10.1016/j.celrep.2015.07.034.

ACKNOWLEDGMENTS

We are grateful to Dr. Anton Valouev for advice on statistical analysis. S.K. was supported by John McKay Fellowship Award from University Kidney Research Organisation, Los Angeles. A.S. was supported by grants from the Agence Nationale de la Recherche (09-Geno-027-01; ANR-11-LABX-0028-01) and the Fondation Recherche Medicale. A.R. was supported by a fellowship from the Fondation Recherche Medicale. Work in A.P.M.'s laboratory was supported by a grant from the California Institute for Regenerative Medicine (LA1-06536).

Received: May 6, 2015
Revised: June 29, 2015
Accepted: July 15, 2015
Published: August 13, 2015

REFERENCES

Abbate, M., Brown, D., and Bonventre, J.V. (1999). Expression of NCAM recapitulates tubulogenic development in kidneys recovering from acute ischemia. Am. J. Physiol. *277*, F454–F463.

Abuelo, J.G. (2007). Normotensive ischemic acute renal failure. N. Engl. J. Med. *357*, 797–805.

Angelotti, M.L., Ronconi, E., Ballerini, L., Peired, A., Mazzinghi, B., Sagrinati, C., Parente, E., Gacci, M., Carini, M., Rotondi, M., et al. (2012). Characterization of renal progenitors committed toward tubular lineage and their regenerative potential in renal tubular injury. Stem Cells *30*, 1714–1725.

Berger, K., and Moeller, M.J. (2014). Mechanisms of epithelial repair and regeneration after acute kidney injury. Semin. Nephrol. *34*, 394–403.

Bonventre, J.V., and Yang, L. (2010). Kidney injury molecule-1. Curr. Opin. Crit. Care *16*, 556–561.

Bonventre, J.V., and Yang, L. (2011). Cellular pathophysiology of ischemic acute kidney injury. J. Clin. Invest. *121*, 4210–4221.

Chawla, L.S., Eggers, P.W., Star, R.A., and Kimmel, P.L. (2014). Acute kidney injury and chronic kidney disease as interconnected syndromes. N. Engl. J. Med. *371*, 58–66.

Chertow, G.M., Burdick, E., Honour, M., Bonventre, J.V., and Bates, D.W. (2005). Acute kidney injury, mortality, length of stay, and costs in hospitalized patients. J. Am. Soc. Nephrol. *16*, 3365–3370.

Cheung, M., and Briscoe, J. (2003). Neural crest development is regulated by the transcription factor Sox9. Development *130*, 5681–5693.

Coca, S.G., Singanamala, S., and Parikh, C.R. (2012). Chronic kidney disease after acute kidney injury: a systematic review and meta-analysis. Kidney Int. *81*, 442–448.

Fabian, S.L., Penchev, R.R., St-Jacques, B., Rao, A.N., Sipilä, P., West, K.A., McMahon, A.P., and Humphreys, B.D. (2012). Hedgehog-Gli pathway activation during kidney fibrosis. Am. J. Pathol. *180*, 1441–1453.

Ferrer-Vaquer, A., Piliszek, A., Tian, G., Aho, R.J., Dufort, D., and Hadjantonakis, A.K. (2010). A sensitive and bright single-cell resolution live imaging reporter of Wnt/ß-catenin signaling in the mouse. BMC Dev. Biol. *10*, 121.

Foster, J.W., Dominguez-Steglich, M.A., Guioli, S., Kwok, C., Weller, P.A., Stevanović, M., Weissenbach, J., Mansour, S., Young, I.D., Goodfellow, P.N., et al. (1994). Campomelic dysplasia and autosomal sex reversal caused by mutations in an SRY-related gene. Nature *372*, 525–530.

Furuyama, K., Kawaguchi, Y., Akiyama, H., Horiguchi, M., Kodama, S., Kuhara, T., Hosokawa, S., Elbahrawy, A., Soeda, T., Koizumi, M., et al. (2011). Continuous cell supply from a Sox9-expressing progenitor zone in adult liver, exocrine pancreas and intestine. Nat. Genet. *43*, 34–41.

Guo, W., Keckesova, Z., Donaher, J.L., Shibue, T., Tischler, V., Reinhardt, F., Itzkovitz, S., Noske, A., Zürrer-Härdi, U., Bell, G., et al. (2012). Slug and Sox9 cooperatively determine the mammary stem cell state. Cell *148*, 1015–1028.

Haase-Fielitz, A., Haase, M., and Devarajan, P. (2014). Neutrophil gelatinase-associated lipocalin as a biomarker of acute kidney injury: a critical evaluation of current status. Ann. Clin. Biochem. *51*, 335–351.

Humphreys, B.D., Valerius, M.T., Kobayashi, A., Mugford, J.W., Soeung, S., Duffield, J.S., McMahon, A.P., and Bonventre, J.V. (2008). Intrinsic epithelial cells repair the kidney after injury. Cell Stem Cell *2*, 284–291.

Humphreys, B.D., Lin, S.L., Kobayashi, A., Hudson, T.E., Nowlin, B.T., Bonventre, J.V., Valerius, M.T., McMahon, A.P., and Duffield, J.S. (2010). Fate tracing reveals the pericyte and not epithelial origin of myofibroblasts in kidney fibrosis. Am. J. Pathol. *176*, 85–97.

Ichimura, T., Bonventre, J.V., Bailly, V., Wei, H., Hession, C.A., Cate, R.L., and Sanicola, M. (1998). Kidney injury molecule-1 (KIM-1), a putative epithelial cell adhesion molecule containing a novel immunoglobulin domain, is up-regulated in renal cells after injury. J. Biol. Chem. *273*, 4135–4142.

Ichimura, T., Asseldonk, E.J., Humphreys, B.D., Gunaratnam, L., Duffield, J.S., and Bonventre, J.V. (2008). Kidney injury molecule-1 is a phosphatidylserine receptor that confers a phagocytic phenotype on epithelial cells. J. Clin. Invest. *118*, 1657–1668.

Imgrund, M., Gröne, E., Gröne, H.J., Kretzler, M., Holzman, L., Schlöndorff, D., and Rothenpieler, U.W. (1999). Re-expression of the developmental gene Pax-2 during experimental acute tubular necrosis in mice 1. Kidney Int. *56*, 1423–1431.

Kamachi, Y., and Kondoh, H. (2013). Sox proteins: regulators of cell fate specification and differentiation. Development *140*, 4129–4144.

Kawaguchi, Y. (2013). Sox9 and programming of liver and pancreatic progenitors. J. Clin. Invest. *123*, 1881–1886.

Kent, J., Wheatley, S.C., Andrews, J.E., Sinclair, A.H., and Koopman, P. (1996). A male-specific role for SOX9 in vertebrate sex determination. Development *122*, 2813–2822.

Kramann, R., and Humphreys, B.D. (2014). Kidney pericytes: roles in regeneration and fibrosis. Semin. Nephrol. *34*, 374–383.

Kumar, S., Allen, D.A., Kieswich, J.E., Patel, N.S., Harwood, S., Mazzon, E., Cuzzocrea, S., Raftery, M.J., Thiemermann, C., and Yaqoob, M.M. (2009). Dexamethasone ameliorates renal ischemia-reperfusion injury. J. Am. Soc. Nephrol. *20*, 2412–2425.

Kumar, S., Liu, J., and McMahon, A.P. (2014). Defining the acute kidney injury and repair transcriptome. Semin. Nephrol. *34*, 404–417.

Kusaba, T., Lalli, M., Kramann, R., Kobayashi, A., and Humphreys, B.D. (2014). Differentiated kidney epithelial cells repair injured proximal tubule. Proc. Natl. Acad. Sci. USA *111*, 1527–1532.

Langworthy, M., Zhou, B., de Caestecker, M., Moeckel, G., and Baldwin, H.S. (2009). NFATc1 identifies a population of proximal tubule cell progenitors. J. Am. Soc. Nephrol. *20*, 311–321.

Lazzeri, E., Crescioli, C., Ronconi, E., Mazzinghi, B., Sagrinati, C., Netti, G.S., Angelotti, M.L., Parente, E., Ballerini, L., Cosmi, L., et al. (2007). Regenerative potential of embryonic renal multipotent progenitors in acute renal failure. J. Am. Soc. Nephrol. *18*, 3128–3138.

Lindoso, R.S., Verdoorn, K.S., and Einicker-Lamas, M. (2009). Renal recovery after injury: the role of Pax-2. Nephrol. Dial. Transplant. *24*, 2628–2633.

Ling, S., Chang, X., Schultz, L., Lee, T.K., Chaux, A., Marchionni, L., Netto, G.J., Sidransky, D., and Berman, D.M. (2011). An EGFR-ERK-SOX9 signaling cascade links urothelial development and regeneration to cancer. Cancer Res. *71*, 3812–3821.

Lindgren, D., Bostrom, A.K., Nilsson, K., Hansson, J., Sjölund, J., Möller, C., Jirström, K., Nilsson, E., Landberg, G., Axelson, H., et al. (2011). Isolation and characterization of progenitor-like cells from human renal proximal tubules. Am. J. Pathol. *178*, 828–837.

Liu, J., Krautzberger, A.M., Sui, S.H., Hofmann, O.M., Chen, Y., Baetscher, M., Grgic, I., Kumar, S., Humphreys, B.D., Hide, W.A., and McMahon, A.P. (2014). Cell-specific translational profiling in acute kidney injury. J. Clin. Invest. *124*, 1242–1254.

Madisen, L., Zwingman, T.A., Sunkin, S.M., Oh, S.W., Zariwala, H.A., Gu, H., Ng, L.L., Palmiter, R.D., Hawrylycz, M.J., Jones, A.R., et al. (2010). A robust and high-throughput Cre reporting and characterization system for the whole mouse brain. Nat. Neurosci. *13*, 133–140.

Mead, T.J., Wang, Q., Bhattaram, P., Dy, P., Afelik, S., Jensen, J., and Lefebvre, V. (2013). A far-upstream (-70 kb) enhancer mediates Sox9 auto-regulation in somatic tissues during development and adult regeneration. Nucleic Acids Res. *41*, 4459–4469.

Mishra, J., Ma, Q., Prada, A., Mitsnefes, M., Zahedi, K., Yang, J., Barasch, J., and Devarajan, P. (2003). Identification of neutrophil gelatinase-associated lipocalin as a novel early urinary biomarker for ischemic renal injury. J. Am. Soc. Nephrol. *14*, 2534–2543.

Nowak, J.A., Polak, L., Pasolli, H.A., and Fuchs, E. (2008). Hair follicle stem cells are specified and function in early skin morphogenesis. Cell Stem Cell *3*, 33–43, Corrected in J. Clin. Invest. 2014;124:2288 (Note: Humphreys, Benjamin [corrected to Humphreys, Benjamin D]).

Oberbauer, R., Rohrmoser, M., Regele, H., Muhlbacher, F., and Mayer, G. (1999). Apoptosis of tubular epithelial cells in donor kidney biopsies predicts early renal allograft function. J. Am. Soc. Nephrol. *10*, 2006–2013.

Poché, R.A., Furuta, Y., Chaboissier, M.C., Schedl, A., and Behringer, R.R. (2008). Sox9 is expressed in mouse multipotent retinal progenitor cells and functions in Müller glial cell development. J. Comp. Neurol. *510*, 237–250.

Reginensi, A., Clarkson, M., Neirijnck, Y., Lu, B., Ohyama, T., Groves, A.K., Sock, E., Wegner, M., Costantini, F., Chaboissier, M.C., and Schedl, A. (2011). SOX9 controls epithelial branching by activating RET effector genes during kidney development. Hum. Mol. Genet. *20*, 1143–1153.

Rinkevich, Y., Montoro, D.T., Contreras-Trujillo, H., Harari-Steinberg, O., Newman, A.M., Tsai, J.M., Lim, X., Van-Amerongen, R., Bowman, A., Januszyk, M., et al. (2014). In vivo clonal analysis reveals lineage-restricted progenitor characteristics in mammalian kidney development, maintenance, and regeneration. Cell Rep. *7*, 1270–1283.

Rizzoti, K., Akiyama, H., and Lovell-Badge, R. (2013). Mobilized adult pituitary stem cells contribute to endocrine regeneration in response to physiological demand. Cell Stem Cell *13*, 419–432.

Romagnani, P. (2011). Family portrait: renal progenitor of Bowman's capsule and its tubular brothers. Am. J. Pathol. *178*, 490–493.

Sarkar, A., and Hochedlinger, K. (2013). The sox family of transcription factors: versatile regulators of stem and progenitor cell fate. Cell Stem Cell *12*, 15–30.

Shakya, R., Watanabe, T., and Costantini, F. (2005). The role of GDNF/Ret signaling in ureteric bud cell fate and branching morphogenesis. Dev. Cell *8*, 65–74.

Smeets, B., Boor, P., Dijkman, H., Sharma, S.V., Jirak, P., Mooren, F., Berger, K., Bornemann, J., Gelman, I.H., Floege, J., et al. (2013). Proximal tubular cells contain a phenotypically distinct, scattered cell population involved in tubular regeneration. J. Pathol. *229*, 645–659.

Soriano, P. (1999). Generalized lacZ expression with the ROSA26 Cre reporter strain. Nat. Genet. *21*, 70–71.

Tata, P.R., Mou, H., Pardo-Saganta, A., Zhao, R., Prabhu, M., Law, B.M., Vinarsky, V., Cho, J.L., Breton, S., Sahay, A., et al. (2013). Dedifferentiation of committed epithelial cells into stem cells in vivo. Nature *503*, 218–223.

Terada, Y., Tanaka, H., Okado, T., Shimamura, H., Inoshita, S., Kuwahara, M., and Sasaki, S. (2003). Expression and function of the developmental gene Wnt-4 during experimental acute renal failure in rats. J. Am. Soc. Nephrol. *14*, 1223–1233.

Villanueva, S., Céspedes, C., and Vio, C.P. (2006). Ischemic acute renal failure induces the expression of a wide range of nephrogenic proteins. Am. J. Physiol. Regul. Integr. Comp. Physiol. *290*, R861–R870.

Wagner, T., Wirth, J., Meyer, J., Zabel, B., Held, M., Zimmer, J., Pasantes, J., Bricarelli, F.D., Keutel, J., Hustert, E., et al. (1994). Autosomal sex reversal and campomelic dysplasia are caused by mutations in and around the SRY-related gene SOX9. Cell *79*, 1111–1120.

Witzgall, R., Brown, D., Schwarz, C., and Bonventre, J.V. (1994). Localization of proliferating cell nuclear antigen, vimentin, c-Fos, and clusterin in the postischemic kidney. Evidence for a heterogenous genetic response among nephron segments, and a large pool of mitotically active and dedifferentiated cells. J. Clin. Invest. *93*, 2175–2188.

Wright, E.M., Snopek, B., and Koopman, P. (1993). Seven new members of the Sox gene family expressed during mouse development. Nucleic Acids Res. *21*, 744.

Wright, E., Hargrave, M.R., Christiansen, J., Cooper, L., Kun, J., Evans, T., Gangadharan, U., Greenfield, A., and Koopman, P. (1995). The Sry-related gene Sox9 is expressed during chondrogenesis in mouse embryos. Nat. Genet. *9*, 15–20.

Zhang, C., Yang, F., Cornelia, R., Tang, W., Swisher, S., and Kim, H. (2011). Hypoxia-inducible factor-1 is a positive regulator of Sox9 activity in femoral head osteonecrosis. Bone *48*, 507–513.